Nonequilibrium Fluctuation-Response Relations: From Identities to Bounds

Timur Aslyamov⊙,[1,*] Krzysztof Ptaszyński⊙,[2,†] and Massimiliano Esposito⊙[1,‡]

[1]*Complex Systems and Statistical Mechanics, Department of Physics and Materials Science,*
University of Luxembourg, 30 Avenue des Hauts-Fourneaux, L-4362 Esch-sur-Alzette, Luxembourg
[2]*Institute of Molecular Physics, Polish Academy of Sciences, Mariana Smoluchowskiego 17, 60-179 Poznań, Poland*

In nonequilibrium steady states of Markov jump processes, we derive exact fluctuation-response relations (FRRs) that express the covariance between any pair of currents in terms of static responses in a notably simple form, thus generalizing the fluctuation-dissipation theorem far from equilibrium. We begin by considering perturbations in the symmetric part of the rates. We demonstrate that FRRs imply a hierarchy of thermodynamic bounds. These hierarchies prove the recently conjectured response thermodynamic uncertainty relation, which bounds the ratio between any current's response and its variance by the entropy production rate (EPR). We furthermore strengthen this bound in two distinct ways, using a partial EPR in one case and a pseudo-EPR in the other. For perturbations in the antisymmetric part of the rates, we show that the ratio between any current's response and its variance is bounded by traffic, a metric representing the total number of transitions per unit time in the system. As an application, we use FRRs to explain the origin of positive correlations between currents in Coulomb-blockaded systems previously observed in experiments.

Introduction—Fluctuations in nonequilibrium steady states (NESSs) of Markov jump processes play a central role in nonequilibrium physics. Close to equilibrium, the seminal fluctuation-dissipation theorem links equilibrium fluctuations to the linear response of a system to external forces [1–5]. This result has been generalized by relating fluctuations to the linear response in a NESS [6–12].

Another, apparently unrelated, result regarding nonequilibrium fluctuations are thermodynamic uncertainty relations (TURs). The original TUR upper bounds the squared precision of current observables (i.e., the ratio between the square of the average current $\mathcal{J}$ and its variance $\langle\langle\mathcal{J}\rangle\rangle$) by half of the entropy production rate (EPR) $\dot{\sigma}$, where the Boltzmann constant $k_B = 1$ [13–23]. A tighter version also replaces $\dot{\sigma}/2$ by the pseudo-EPR [24]. Another inequality, the kinetic uncertainty relation (KUR), bounds the squared precision by traffic, a quantity that measures the total number of transitions per unit time in the system [25].

A first connection between responses and TURs was obtained in [21,22] by upper bounding the ratio of the squared difference between a perturbed and unperturbed average observable to its unperturbed variance by twice the Kullback-Leibler divergence between the perturbed and unperturbed path probability taken by the system. This bound was tightened in [26] and asymmetric response

relations were also obtained. Recently, a more explicit connection was found with the response-TUR (R-TUR) conjectured in [27], but it has not been proven so far. This result upper bounds the precision of kinetic perturbations to currents (i.e., the ratio between the squared static response of a current to perturbations of kinetic barriers and the current variance) by half the EPR multiplied by the squared maximal rate of change of kinetic barriers in the system. Thus, it relates response, fluctuations, and dissipation in the form of a bound, raising the important question of whether an exact relation exists between these quantities.

In this Letter, we derive such exact relations and coin them "fluctuation-response relations" (FRRs). They relate the covariance between two arbitrary currents to their static responses to arbitrary perturbations of the transition rate matrix. Hierarchies of thermodynamic bounds can be derived from them. For symmetric perturbations of the rates, we not only prove the R-TUR conjectured in [27], but also tighten them in terms of partial-EPRs and pseudo-EPRs. For antisymmetric perturbations of the rates, we find a related hierarchy of response-KUR (R-KUR) bounds, but this time in terms of traffic rather than entropy production. We also show that FRRs straightforwardly imply the original TUR as well its pseudo-EPR and kinetic versions. Finally, we apply FRRs to explain the origin of positive correlations in the currents across a double quantum dot setup measured in the Coulomb-blockade regime.

Setup—We consider a continuous-time Markov jump process among N discrete states. In NESS we have

---

*Contact author: timur.aslyamov@uni.lu
†Contact author: krzysztof.ptaszynski@ifmpan.poznan.pl
‡Contact author: massimiliano.esposito@uni.lu

$$d_t \boldsymbol{\pi} = \mathbb{W} \cdot \boldsymbol{\pi} = 0, \tag{1}$$

where $\boldsymbol{\pi} = (\dots, \pi_n, \dots)^\intercal$ is the vector of state probabilities π_n with $\sum_n \pi_n = 1$. The matrix $\mathbb{W}$ is the rate matrix with off-diagonal elements $W_{nm} = \sum_e [W_{+e} \delta_{s(+e)m} \delta_{t(+e)n} + W_{-e} \delta_{s(+e)n} \delta_{t(+e)m}]$, where $s(\pm e)$ is the source of edge $\pm e$, and $t(\pm e)$ is the target of edge $\pm e$, and diagonal elements $W_{nn} = -\sum_{m \neq n} W_{mn}$. Every transition rate can be generically parametrized as

$$W_{\pm e} = \exp[B_e \pm S_e/2], \tag{2}$$

where B_e and S_e parametrize the symmetric and antisymmetric part of the transition rate, respectively. For physical systems in contact with thermal reservoirs (rates that satisfy the local detailed balance), the term B_e characterizes the kinetic barriers that can be controlled by varying catalyst concentrations (e.g., enzymes) [28], applying magnetic fields (e.g., via the radical pair mechanism in magnetoreception) [29–32], adjustment of tunnel barriers [33–35], or potential barriers [36,37] by gate voltages in nanoelectronics, while the term S_e, is the change in entropy in the reservoir due to a transition e that includes changes in thermodynamic forces and energy landscape [38–40]. The current through the edge e is $j_e = W_{+e} \pi_{s(+e)} - W_{-e} \pi_{t(+e)}$; all unoriented transitions through the edge e are characterized by a traffic $\tau_e = W_{+e} \pi_{s(+e)} + W_{-e} \pi_{t(+e)}$. The dissipation in the system is defined by the total EPR, $\dot{\sigma} = \sum_e \dot{\sigma}_e$, where $\dot{\sigma}_e = j_e \ln(W_{+e} \pi_{s(+e)} / W_{-e} \pi_{t(+e)})$ is the single edge EPR. A steady state is an equilibrium if $\dot{\sigma} = 0$ (and thus all $j_e = 0$) and a NESS if $\dot{\sigma} > 0$.

To characterize the average and fluctuations of current observables, we introduce the stochastic counting variable $k_e(t) = k_{+e}(t) - k_{-e}(t)$, where $k_{\pm e}(t)$ is the number of jumps in the direction $\pm e$ during the time interval $[0,t]$. The average of an arbitrary current observable $\mathcal{J}$ is given by

$$\mathcal{J} \equiv \lim_{t \to \infty} t^{-1} \left\langle \sum_e x_e k_e(t) \right\rangle = \sum_e x_e j_e, \tag{3}$$

where $\boldsymbol{x} = (\dots, x_e, \dots)^\intercal$ is an arbitrary vector. The covariance between two arbitrary current observables $\langle\!\langle \mathcal{J}, \mathcal{J}' \rangle\!\rangle$, where $\mathcal{J}' = \sum_e x'_e j_e$ with $\boldsymbol{x}' = (\dots, x'_e, \dots)^\intercal$, is in turn

$$\langle\!\langle \mathcal{J}, \mathcal{J}' \rangle\!\rangle \equiv \lim_{t \to \infty} t^{-1} \left\langle \sum_e x_e \Delta k_e(t) \sum_{e'} x_{e'} \Delta k_{e'}(t) \right\rangle = \boldsymbol{x}^\intercal \mathbb{C} \boldsymbol{x}', \tag{4}$$

where $\Delta k_e(t) = k_e(t) - \langle k_e(t) \rangle$ and $\mathbb{C}$ is the covariance matrix of edge currents with elements $C_{ee'} = \lim_{t \to \infty} t^{-1} \langle \Delta k_e(t) \Delta k_{e'}(t) \rangle$. The exact expression for the covariance matrix $\mathbb{C}$ is given in Eq. (A2) in Appendix A.

Fluctuation-response relations—These are derived in detail in Appendix A. They link the covariance of currents

to the static response of currents to perturbations in the rates. The term "static response" means that one considers the linear response of the steady-state currents to the perturbation of the rates [41]. From an operational perspective, it corresponds to measuring the current responses for a sufficiently long time after introducing the perturbation of the rates, so that the system has relaxed to the new stationary state. In the main text, we assume that the vector $\boldsymbol{x}$ does not depend on the perturbation parameter, resulting in static responses of the current observable $\mathcal{J}$ as $d_{B_e} \mathcal{J} = \sum_{e'} x_{e'} d_{B_e} j_{e'}$ and $d_{S_e} \mathcal{J} = \sum_{e'} x_{e'} d_{S_e} j_{e'}$, where $d_p j_e [p, \boldsymbol{\pi}(p)] = \partial_p j_e + \sum_n \partial_{\pi_n} j_e \partial_p \pi_n$, with $p \in \{B_e, S_e\}$. The results for an arbitrary $\boldsymbol{x}$ are shown in Appendix A.

For symmetric perturbations, B_e, the FRR reads

$$\langle\!\langle \mathcal{J}, \mathcal{J}' \rangle\!\rangle = \nabla_B^\intercal \mathcal{J} \cdot \mathbb{D}^{-1} \cdot \nabla_B \mathcal{J}' = \sum_e \frac{\tau_e}{j_e^2} d_{B_e} \mathcal{J} d_{B_e} \mathcal{J}'. \tag{5}$$

Here, $\nabla_B \mathcal{J} = (\dots, d_{B_e} \mathcal{J}, \dots)^\intercal$ and $\mathbb{D} = \text{diag}(\dots, j_e^2/\tau_e, \dots)$ is the diagonal matrix with the pseudo-EPR as trace, $\dot{\Pi} = \text{tr}\mathbb{D} = \sum_e j_e^2/\tau_e$. The pseudo-EPR is a measure of irreversibility (nonnegative and zero at equilibrium). It coincides with $\dot{\sigma}/2$ close to equilibrium $[\dot{\sigma}_e/2 = j_e \text{arctanh}(j_e/\tau_e) = j_e^2/\tau_e + \mathcal{O}(j_e^4)]$ and plays an important role in the generalization of TURs [24,42–44]. The current variance $\langle\!\langle \mathcal{J} \rangle\!\rangle$ is obtained from Eq. (5) when $\mathcal{J} = \mathcal{J}'$ as

$$\langle\!\langle \mathcal{J} \rangle\!\rangle = \sum_e \frac{\tau_e}{j_e^2} (d_{B_e} \mathcal{J})^2. \tag{6}$$

For antisymmetric perturbations, S_e, the FRR for the covariance reads

$$\langle\!\langle \mathcal{J}, \mathcal{J}' \rangle\!\rangle = 4 \nabla_S^\intercal \mathcal{J} \cdot \mathbb{T}^{-1} \cdot \nabla_S \mathcal{J}' = \sum_e \frac{4}{\tau_e} d_{S_e} \mathcal{J} d_{S_e} \mathcal{J}', \tag{7}$$

and the FRR for the variance is

$$\langle\!\langle \mathcal{J} \rangle\!\rangle = \sum_e \frac{4}{\tau_e} (d_{S_e} \mathcal{J})^2. \tag{8}$$

Here, $\nabla_S \mathcal{J} = (\dots, d_{S_e} \mathcal{J}, \dots)^\intercal$, and $\mathbb{T} = \text{diag}(\dots, \tau_e, \dots)$ is a diagonal matrix with total traffic as trace, $\mathcal{T} = \text{tr}\mathbb{T} = \sum_e \tau_e$. Note that even for single edge currents, $\mathcal{J} = j_e$, the right-hand sides of Eqs. (5)–(8) include contributions from all edges of the network. We note that Eqs. (5) and (6) still hold at a stalling edge where both the denominator, j_e, and the numerator, $\tau_e d_{B_e} \mathcal{J} d_{B_e} \mathcal{J}'$, tend to zero, because their ratio remains finite [41].

FRRs close to equilibrium—We now parametrize the antisymmetric part of Eq. (2) as $S_e = F_e + E_{s(+e)} - E_{t(+e)}$, where E_n can be interpreted as state energies and F_e as nonconservative thermodynamic forces [38]. At steady state $\dot{\sigma} = \boldsymbol{j}^\intercal \boldsymbol{F}$, where $\boldsymbol{F} = (\dots, F_e, \dots)^\intercal$. For $\boldsymbol{F} = \boldsymbol{0}$, the system

steady state is an equilibrium state $\pi_n^{\mathrm{eq}} = \exp(-E_n)/\sum_m \exp(-E_m)$. In the close-to-equilibrium regime, the forces F_e are small. Currents can be linearly expanded in forces as $\boldsymbol{j} = \mathbb{L}\boldsymbol{F}$, where $\mathbb{L} = \mathbb{L}^\intercal$ is the positive semidefinite Onsager matrix; see the explicit form in [45] and [46]. Comparing, on one hand, the response calculated as $\mathcal{J} = \boldsymbol{x}^\intercal \mathbb{L}\boldsymbol{F} \rightarrow \nabla_S^\intercal \mathcal{J}|_{F=0} = \boldsymbol{x}^\intercal \mathbb{L}$ and, on the other hand, the response calculated by Eq. (A4) as $\nabla_S^\intercal \mathcal{J}|_{F=0} = \frac{1}{2}\boldsymbol{x}^\intercal \mathbb{P}^{\mathrm{eq}} \mathbb{T}_{\mathrm{eq}}$, we find $\mathbb{L} = \frac{1}{2}\mathbb{P}_{\mathrm{eq}} \mathbb{T}_{\mathrm{eq}}$, where $\mathbb{P}_{\mathrm{eq}}$ is the equilibrium projection matrix ($\mathbb{P}_{\mathrm{eq}}^2 = \mathbb{P}_{\mathrm{eq}}$); see Eq. (A3). Inserting this expression for the response into Eq. (7), we find

$$\langle\!\langle \mathcal{J} \rangle\!\rangle_{\mathrm{eq}} = \boldsymbol{x}^\intercal \mathbb{P}_{\mathrm{eq}} \mathbb{T}_{\mathrm{eq}} \mathbb{P}_{\mathrm{eq}}^\intercal \boldsymbol{x} = \boldsymbol{x}^\intercal \mathbb{P}_{\mathrm{eq}}^2 \mathbb{T}_{\mathrm{eq}} \boldsymbol{x} = \boldsymbol{x}^\intercal 2\mathbb{L}\boldsymbol{x}, \quad (9)$$

where we used $2\mathbb{L} = \mathbb{P}_{\mathrm{eq}} \mathbb{T}_{\mathrm{eq}} = \mathbb{T}_{\mathrm{eq}} \mathbb{P}_{\mathrm{eq}}^\intercal = 2\mathbb{L}^\intercal$. From Eq. (9), we find that equilibrium covariance matrix $\mathbb{C}_{\mathrm{eq}} = 2\mathbb{L}$, which is the fluctuation-dissipation theorem [45]. Using $\boldsymbol{x} = \boldsymbol{F}$, we consider the EPR as the current observable $\dot{\sigma} = \boldsymbol{F}^\intercal \boldsymbol{j} = \boldsymbol{F}^\intercal \mathbb{L}\boldsymbol{F}$. Inserting $\boldsymbol{x} = \boldsymbol{F}$ and $\mathcal{J} = \dot{\sigma}$ in Eq. (9), we also find $\langle\!\langle \dot{\sigma} \rangle\!\rangle_{\mathrm{eq}} = 2\boldsymbol{F}^\intercal \mathbb{L}\boldsymbol{F} = 2\dot{\sigma}$ [15]. In Sec. SIII of [47], we show that the FRR can also be used to derive the fluctuation-dissipation relation valid far from equilibrium but at stalling, originally derived in [9].

Proving and generalizing R-TUR—We now show how FRRs can be used to derive thermodynamic bounds. We introduce the parameters ε and η, which respectively control $B_e(\varepsilon)$ and $S_e(\eta)$, and the current responses

$$d_\varepsilon \mathcal{J} = \sum_e b_e d_{B_e} \mathcal{J}, \qquad d_\eta \mathcal{J} = \sum_e z_e d_{S_e} \mathcal{J}, \quad (10)$$

with perturbation rates $b_e = \partial_\varepsilon B_e$ and $z_e = \partial_\eta S_e$.

Two hierarchies of bounds are derived by combining Eq. (10) with the FRRs (6) and (8), respectively. For the first hierarchy, we use Jensen's inequality to prove $2(a-b)^2/(a+b) \le (a-b)\ln(a/b)$, which implies that $\tau_e/j_e^2 \ge 2/\dot{\sigma}_e$, and from Eq. (6), we arrive at

$$\langle\!\langle \mathcal{J} \rangle\!\rangle \ge \sum_e \frac{2}{\dot{\sigma}_e}(d_{B_e}\mathcal{J})^2 = \sum_e \frac{2}{b_e^2 \dot{\sigma}_e}(b_e d_{B_e}\mathcal{J})^2. \quad (11)$$

Sedrakyan's inequality, $\sum_i a_i^2/b_i \ge (\sum_i a_i)^2/(\sum_i b_i)$, which holds for real a_i and positive b_i, implies

$$\sum_e \frac{(b_e d_{B_e}\mathcal{J})^2}{b_e^2 \dot{\sigma}_e} \ge \frac{(\sum_e b_e d_{B_e}\mathcal{J})^2}{\sum_e b_e^2 \dot{\sigma}_e} = \frac{(d_\varepsilon \mathcal{J})^2}{\sum_e b_e^2 \dot{\sigma}_e}, \quad (12)$$

where we used Eq. (10) for the last equality. Noticing that

$$\sum_e b_e^2 \dot{\sigma}_e = b_{\max}^2 \dot{\sigma}_\beta \le b_{\max}^2 \dot{\sigma}_\omega \le b_{\max}^2 \dot{\sigma}, \quad (13)$$

where $b_{\max} = \max_e |b_e|$, $\dot{\sigma}_\beta \equiv \sum_e \beta_e^2 \dot{\sigma}_e$ is the weighted EPR with $\beta_e = b_e/b_{\max}$, $\dot{\sigma}_\omega$ is the partial EPR [52] for the

set ω of perturbed edges (i.e., the set of edges for which $b_e \ne 0$), and where we used $\beta_e^2 \le 1$ for the first inequality. Intuitively, $b_{\max}$ characterizes the most abrupt change in barriers resulting from a perturbation in the physical parameter. Inserting Eqs. (10), (12), and (13) in Eq. (11) we find the first hierarchy

$$\frac{(d_\varepsilon \mathcal{J})^2}{b_{\max}^2 \langle\!\langle \mathcal{J} \rangle\!\rangle} = \frac{(\sum_e \beta_e d_{B_e}\mathcal{J})^2}{\langle\!\langle \mathcal{J} \rangle\!\rangle} \le \frac{\dot{\sigma}_\beta}{2} \le \frac{\dot{\sigma}_\omega}{2} \le \frac{\dot{\sigma}}{2}, \quad (14)$$

which proves and generalizes the R-TUR conjectured in [27]. Using the fact that for single edge perturbation $\varepsilon = B_e$ and thus $b_{\max} = 1$, we find

$$\frac{(d_{B_e}\mathcal{J})^2}{\langle\!\langle \mathcal{J} \rangle\!\rangle} \le \frac{\dot{\sigma}_e}{2}, \quad (15)$$

which bounds the response by the single edge EPR. Since Eq. (14) holds for arbitrary β_e, using $\beta_e = \mathrm{sign}\, d_{B_e}\mathcal{J}$ for the last inequality in Eq. (14), we also find the bound

$$\frac{(\sum_e |d_{B_e}\mathcal{J}|)^2}{\langle\!\langle \mathcal{J} \rangle\!\rangle} \le \frac{\dot{\sigma}}{2}, \quad (16)$$

which is tighter than the bound derived from the edge summation of Eq. (15).

To derive the second hierarchy, we start from Eq. (8)

$$\frac{\langle\!\langle \mathcal{J} \rangle\!\rangle}{4} = \sum_e \frac{(z_e d_{S_e}\mathcal{J})^2}{z_e^2 \tau_e} \ge \frac{(\sum_e z_e d_{S_e}\mathcal{J})^2}{\sum_e z_e^2 \tau_e} = \frac{(d_\eta \mathcal{J})^2}{\sum_e z_e^2 \tau_e}, \quad (17)$$

where we used Sedrakyan's inequality and Eq. (10) for the last equality. As for Eq. (13), we have

$$\sum_e z_e^2 \tau_e = z_{\max}^2 \mathcal{T}_\zeta \le z_{\max}^2 \mathcal{T}_\varphi \le z_{\max}^2 \mathcal{T}, \quad (18)$$

which, with Eq. (17), results in the R-KUR hierarchy

$$\frac{(d_\eta \mathcal{J})^2}{z_{\max}^2 \langle\!\langle \mathcal{J} \rangle\!\rangle} = \frac{(\sum_e \zeta_e d_{S_e}\mathcal{J})^2}{\langle\!\langle \mathcal{J} \rangle\!\rangle} \le \frac{\mathcal{T}_\zeta}{4} \le \frac{\mathcal{T}_\varphi}{4} \le \frac{\mathcal{T}}{4}, \quad (19)$$

where $z_{\max} = \max_e |z_e|$, $\mathcal{T}_\zeta = \sum_e \zeta_e^2 \tau_e$ is the weighted traffic with $\zeta_e = z_e/z_{\max}$, and $\mathcal{T}_\varphi = \sum_{e \in \varphi} \tau_e$ for the set φ defining the perturbed edges ($z_e \ne 0$). We note that the hierarchy of bounds in Eq. (19) can be alternatively obtained using information geometry approach [53]. Since $\eta = S_e$ implies $z_{\max} = 1$, using Eq. (19), we obtain the single edge R-KUR

$$\frac{(d_{S_e}\mathcal{J})^2}{\langle\!\langle \mathcal{J} \rangle\!\rangle} \le \frac{\tau_e}{4}. \quad (20)$$

Repeating the procedure leading to Eq. (16), the last inequality in Eq. (19) can be rewritten as

$$\frac{(\sum_e |d_{S_e} \mathcal{J}|)^2}{\langle\langle \mathcal{J} \rangle\rangle} \le \frac{\mathcal{T}}{4}, \tag{21}$$

which is tighter than the one derived from the edge summation of Eq. (20).

Introducing the squared precision $\phi = \mathcal{J}^2 / \langle\langle \mathcal{J} \rangle\rangle$ and the sensitivity of the current observable $d_p \ln \mathcal{J} \equiv d_p \mathcal{J} / \mathcal{J}$, the single edge R-TURs, Eqs. (15) and (20), take the compact form

$$\sigma_e \ge 2(d_{B_e} \ln \mathcal{J})^2 \phi, \qquad \tau_e \ge 4(d_{S_e} \ln \mathcal{J})^2 \phi. \tag{22}$$

These results show that dissipation and traffic impose a trade-off between precision and sensitivity.

Pseudo-EPR forms of R-TUR and TUR—Multiplying both sides of Eq. (6) by $\dot{\Pi}$ and using the Cauchy-Schwarz inequality $(\sum_i a_i^2)(\sum_i b_i^2) \ge (\sum_i |a_i b_i|)^2$, we arrive at

$$\dot{\Pi} \langle\langle \mathcal{J} \rangle\rangle = \left(\sum_e \frac{j_e^2}{\tau_e} \right) \sum_e (d_{B_e} \mathcal{J})^2 \frac{\tau_e}{j_e^2} \ge \left(\sum_e |d_{B_e} \mathcal{J}| \right)^2. \tag{23}$$

We note that since $\dot{\Pi} \le \dot{\sigma}/2$, the bound in Eq. (23) is tighter than Eq. (16). Since the response $d_\varepsilon \mathcal{J}$ in Eq. (10) is bounded as

$$(d_\varepsilon \mathcal{J})^2 = \left(\sum_e b_e d_{B_e} \mathcal{J} \right)^2 \le b_{\max}^2 \left(\sum_e |d_{B_e} \mathcal{J}| \right)^2, \tag{24}$$

using Eqs. (23) and (24) together with $\dot{\Pi} \le \dot{\sigma}/2$, we find

$$\frac{(d_\varepsilon \mathcal{J})^2}{\langle\langle \mathcal{J} \rangle\rangle} \le b_{\max}^2 \dot{\Pi} \le \frac{b_{\max}^2 \dot{\sigma}}{2}. \tag{25}$$

By bounding the precision of current response to symmetric perturbations using the pseudo-EPR instead of the EPR, this result constitutes a tighter version of the R-TUR.

To recover the standard TUR, we relax Eq. (23) by omitting the absolute value inside summations,

$$\dot{\Pi} \langle\langle \mathcal{J} \rangle\rangle \ge \left(\sum_e d_{B_e} \mathcal{J} \right)^2 = \mathcal{J}^2, \tag{26}$$

where in the last step we used $\sum_e d_{B_e} j_{e'} = j_{e'}$, which is a special case of the summation response relations [54]. From Eq. (26), we find

$$\frac{\mathcal{J}^2}{\langle\langle \mathcal{J} \rangle\rangle} \le \dot{\Pi} \le \frac{\dot{\sigma}}{2}. \tag{27}$$

For the standard TUR, our derivation of Eq. (27) is complementary to the method [24] based on the Cramér-Rao inequality and Fisher information; see also [43,44]. The second inequalities in Eqs. (25) and (27) are saturated if and only if $j_e^2 / \tau_e = \dot{\sigma}_e / 2$ for $\forall e$, namely close to

equilibrium. It explains the simulations in Ref. [27] observing tight bounds only close to equilibrium, even for optimized TUR and R-TUR. Furthermore, since $j_e \le \tau_e$, we find that $\dot{\Pi} \le \mathcal{T}$, which using Eqs. (25) and (27) implies that

$$\frac{(d_\varepsilon \mathcal{J})^2}{\langle\langle \mathcal{J} \rangle\rangle} \le b_{\max}^2 \mathcal{T}, \qquad \frac{\mathcal{J}^2}{\langle\langle \mathcal{J} \rangle\rangle} \le \mathcal{T}. \tag{28}$$

The right inequality is the kinetic-TUR derived in [25] using the method of [21]. The left inequality constitutes a kinetic version of the R-TUR.

Application of FRRs—We consider two examples illustrating our approach: the Coulomb-blockaded system based on the quantum dots in the main text and chemical reactions obeying mass action law in Appendix B. Both examples show how perturbations in FRRs can be controlled by the physical parameters. The quantum dots example focuses on the analysis of the exact FRR. In the chemical example, we discuss the inference of the EPR and traffic. There, analogously to standard TURs and KURs, we use R-TURs and R-KURs to infer the minimum value of the EPR or of traffic using current fluctuations and responses. We illustrate that the EPR and traffic can be inferred using only partial rather than full knowledge of the model. Furthermore, we derive the bounds for the reaction activity and the ratio of the concentrations of chemical species that have recently attracted attention [55–57].

In the context of the quantum dot example, we show that FRRs explain the observation, made in [58,59], of positive cross-correlations in Coulomb-blockaded systems, which are normally negative. To do so we consider the dynamical channel blockade model [60,61]. This model consists of two single level quantum dots (QDs) with energy levels $\epsilon_u = \epsilon_d = 0$. The QDs exchange electrons with two electrodes (reservoirs), which have the same temperature T and chemical potentials $\mu_L = -\mu_R = V/2$, creating a bias V for the left to right; see Fig. 1(a). Electron transitions between the two QDs are impossible, but the two occupied QDs interact with each other through a Coulomb repulsion energy E_C. We consider the limit of $E_C \gg \{V, k_B T\}$ where the probability of finding both QDs filled is negligible. Thus, the Markov network for this model consists of three states (both QDs are empty, u is filled but not d, and vice versa); see the graph in Fig. 1(b). The transition rates assigned to the edges $e \in \{1, 2, 3, 4\}$ are $W_{\pm e} = \Gamma_e \{1 + \exp[\mp V/(2 k_B T)]\}^{-1}$, where Γ_e are the tunneling rates. Therefore, the symmetric parameters $B_e = \ln \sqrt{W_{+e} W_{-e}}$ depend on both Γ_e and V, while the antisymmetric parameters $S_e = \ln(W_{+e}/W_{-e}) = V/(2 k_B T)$ depend only on V. Thus, to perturb only the symmetric parameters, one needs to control the tunneling rates Γ_e. To study the covariance $C_{24} \equiv \langle\langle j_2, j_4 \rangle\rangle$, describing correlations between the different currents on the right electrode, we use the FRR (5) for symmetric perturbations (parameters B_e),
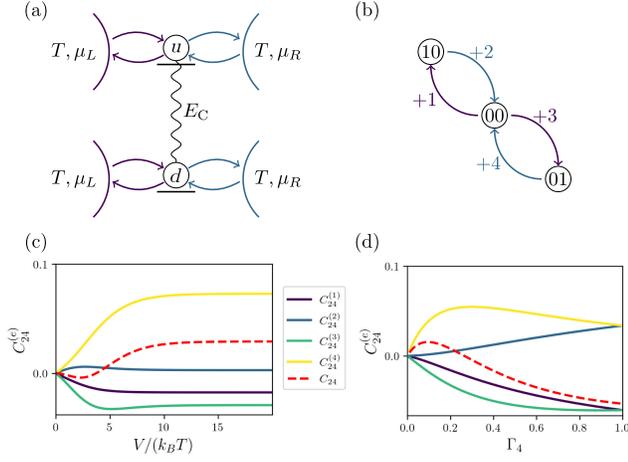
FIG. 1. (a) The scheme of two QDs, u and d (up and down), where every QD is connected to the left and right electrodes (L and R) with temperature T and chemical potentials $\mu_L = -\mu_R = V/2$. Purple and blue arrows depict the electron transfer between QDs and the left and right electrodes, respectively. Wavy curve depicts the Coulomb repulsion with energy E_C between filled QDs. (b) The corresponding Markov network in the limit $E_C \gg \{V, k_B T\}$ with three states: 00, QDs are empty; 10 or 01, only the up or down QD is filled. The arrows depict the directed jumps between the states. Purple and blue arrows are assigned to left and right electrodes, respectively. (c) Dashed red line shows the covariance $C_{24} \equiv \langle\langle j_2, j_4 \rangle\rangle$ as function of the nondimensional potential $V/(k_B T)$ calculated via Eq. (29) for $\Gamma_1 = \Gamma_2 = \Gamma_3 = 1$ and $\Gamma_4 = 0.2$. Colored solid curves are four terms from the left side of Eq. (29), where purple, blue, green, yellow correspond to $e \in \{1, 2, 3, 4\}$, respectively. (d) The same as in (c), but functions of Γ_4 with $V = 5k_B T$.

$$C_{24} = \sum_{e=1}^{4} \frac{\tau_e}{j_e^2} d_{B_e} j_2 d_{B_e} j_4 = \sum_{e=1}^{4} C_{24}^{(e)}, \qquad (29)$$

where $C_{24}^{(e)}$ are the contributions to the covariance from the edge responses. In Sec. SIV of [47] we derive the following inequalities for the terms in Eq. (29):

$$C_{24}^{(1)} \leq 0, \qquad C_{24}^{(2)} \geq 0, \qquad C_{24}^{(3)} \leq 0, \qquad C_{24}^{(4)} \geq 0, \qquad (30)$$

which indicate that the positive correlations originate from the current responses to the perturbation of coupling to the right electrode (the barriers $\{B_2, B_4\}$). The summation of the terms of different signs in Eq. (29) makes both positive and negative correlations C_{24} possible. This can be seen in Figs. 1(c) and 1(d), where we plot the terms of Eq. (29) as functions of the bias V in Fig. 1(c), and the tunneling rate Γ_4 in Fig. 1(d). We see a positive covariance between the currents for sufficiently small rate Γ_4 and large potential V.

Conclusions—FRRs in Eqs. (5)–(8) reveal a fundamental and general relation between static response and fluctuations giving rise to hierarchies of R-TURs and R-KURs. These findings are relevant to any domain utilizing Markov jump processes, as well as the growing body of research on static responses in nonequilibrium systems [40,41,53,62–78]. Static response is crucial for understanding transport properties in nanoelectronic devices, such as quantum dots, where it helps characterize responses to changes in tunneling barriers or voltage biases [33–35], and in CMOS devices subject to shifts in potential barriers or voltage biases [36,37]. In biochemistry, static response plays a pivotal role in quantifying processes like proofreading and sensing [40,67,79], and in analyzing how metabolic fluxes shift due to changes in enzyme concentrations, as seen in metabolic control analysis [80], or to changes in thermodynamic forces [65]. Furthermore, static response is instrumental in optimizing loss functions in nonequilibrium physical computing [72,74]. Future studies may concern the application of FRRs in the context of EPR and traffic inference [81,82], non-Markovian processes [83,84], dynamic responses [85,86], and continuous-space Langevin dynamics [75,76].

Note added—We notice that, the authors of [53] used information theory to derive the R-KUR bound for arbitrary trajectory observables (including current observables) at the transient regime. However, this result does not provide exact FRRs and does not cover the R-TUR. Also, several works related to the present Letter have recently appeared. On the one hand, at the level of static response, we extended FRRs to state-based observables in [87], and the authors of [88] generalized this FRR to "strong perturbations." On the other hand, R-KURs have been generalized to discrete-time Markov processes [89] or open quantum systems [90–92]. Additionally, Ref. [90] provided an alternative proof of the R-TUR [our Eq. (15)], and generalized it to state observables, as well as to transient regimes. We emphasize that the fluctuation-response relations (FRRs) for covariance, which constitute the primary contribution of our Letter, are identities that cannot be obtained using the approaches of Refs. [53,89–92], which are based on the Cramér-Rao inequality that bounds covariances.

[1] R. Kubo, Rep. Prog. Phys. **29**, 255 (1966).
[2] R. Kubo, M. Toda, and N. Hashitsume, *Statistical Physics II: Nonequilibrium Statistical Mechanics* (Springer Science & Business Media, New York, 2012), Vol. 31.
[3] R. L. Stratonovich, *Nonlinear Nonequilibrium Thermodynamics I: Linear and Nonlinear Fluctuation-Dissipation*

Theorems (Springer Science & Business Media, New York, 2012), Vol. 57.

[4] U. M. B. Marconi, A. Puglisi, L. Rondoni, and A. Vulpiani, Phys. Rep. **461**, 111 (2008).

[5] D. Forastiere, R. Rao, and M. Esposito, New J. Phys. **24**, 083021 (2022).

[6] G. S. Agarwal, Z. Phys. A **252**, 25 (1972).

[7] U. Seifert and T. Speck, Europhys. Lett. **89**, 10007 (2010).

[8] J. Prost, J. F. Joanny, and J. M. R. Parrondo, Phys. Rev. Lett. **103**, 090601 (2009).

[9] B. Altaner, M. Polettini, and M. Esposito, Phys. Rev. Lett. **117**, 180601 (2016).

[10] H.-M. Chun, Q. Gao, and J. M. Horowitz, Phys. Rev. Res. **3**, 043172 (2021).

[11] M. Baiesi, C. Maes, and B. Wynants, Phys. Rev. Lett. **103**, 010602 (2009).

[12] N. Shiraishi, *Fundamental Theories of Physics* (Springer, Singapore, 2023).

[13] A. C. Barato and U. Seifert, Phys. Rev. Lett. **114**, 158101 (2015).

[14] T. R. Gingrich, J. M. Horowitz, N. Perunov, and J. L. England, Phys. Rev. Lett. **116**, 120601 (2016).

[15] P. Pietzonka, A. C. Barato, and U. Seifert, Phys. Rev. E **93**, 052145 (2016).

[16] P. Pietzonka, F. Ritort, and U. Seifert, Phys. Rev. E **96**, 012101 (2017).

[17] J. M. Horowitz and T. R. Gingrich, Phys. Rev. E **96**, 020103 (R) (2017).

[18] G. Falasco, M. Esposito, and J.-C. Delvenne, New J. Phys. **22**, 053046 (2020).

[19] J. M. Horowitz and T. R. Gingrich, Nat. Phys. **16**, 15 (2020).

[20] T. Van Vu, V. T. Vo, and Y. Hasegawa, Phys. Rev. E **101**, 042138 (2020).

[21] A. Dechant and S.-i. Sasa, Proc. Natl. Acad. Sci. U.S.A. **117**, 6430 (2020).

[22] A. Dechant and S. ichi Sasa, arXiv:1804.08250.

[23] T. Van Vu and K. Saito, Phys. Rev. X **13**, 011013 (2023).

[24] N. Shiraishi, J. Stat. Phys. **185**, 19 (2021).

[25] I. Di Terlizzi and M. Baiesi, J. Phys. A **52**, 02LT03 (2018).

[26] G. Falasco, M. Esposito, and J.-C. Delvenne, J. Phys. A **55**, 124002 (2022).

[27] K. Ptaszyński, T. Aslyamov, and M. Esposito, Phys. Rev. Lett. **133**, 227101 (2024).

[28] A. Wachtel, R. Rao, and M. Esposito, New J. Phys. **20**, 042002 (2018).

[29] T. Ritz, S. Adem, and K. Schulten, Biophys. J. **78**, 707 (2000).

[30] P. J. Hore and H. Mouritsen, Annu. Rev. Biophys. **45**, 299 (2016).

[31] R. Wiltschko and W. Wiltschko, J. R. Soc. Interface **16**, 20190295 (2019).

[32] H. Zadeh-Haghighi and C. Simon, J. R. Soc. Interface **19**, 20220325 (2022).

[33] S. Gustavsson, R. Leturcq, B. Simovič, R. Schleser, T. Ihn, P. Studerus, K. Ensslin, D. C. Driscoll, and A. C. Gossard, Phys. Rev. Lett. **96**, 076605 (2006).

[34] S. Gustavsson, R. Leturcq, M. Studer, I. Shorubalko, T. Ihn, K. Ensslin, D. Driscoll, and A. Gossard, Surf. Sci. Rep. **64**, 191 (2009).

[35] R. Sánchez, P. Samuelsson, and P. P. Potts, Phys. Rev. Res. **1**, 033066 (2019).

[36] N. Freitas, J.-C. Delvenne, and M. Esposito, Phys. Rev. X **11**, 031064 (2021).

[37] A. Gopal, M. Esposito, and N. Freitas, Phys. Rev. B **106**, 155303 (2022).

[38] R. Rao and M. Esposito, New J. Phys. **20**, 023007 (2018).

[39] G. Falasco and M. Esposito, Rev. Mod. Phys. **97**, 015002 (2025).

[40] J. A. Owen, T. R. Gingrich, and J. M. Horowitz, Phys. Rev. X **10**, 011066 (2020).

[41] T. Aslyamov and M. Esposito, Phys. Rev. Lett. **133**, 107103 (2024).

[42] A. Dechant and S.-I. Sasa, Phys. Rev. X **11**, 041061 (2021).

[43] V. Tuan Vo, T. Van Vu, and Y. Hasegawa, J. Phys. A **55**, 405004 (2022).

[44] A. Dechant, J. Phys. A **55**, 094001 (2022).

[45] H. Vroylandt, D. Lacoste, and G. Verley, J. Stat. Mech. (2019) 054002.

[46] See Appendix B in [27].

[47] See Supplemental Material at http://link.aps.org/supplemental/10.1103/PhysRevLett.134.157101 for (SI) derivation of Eq. (A2), (SII) analysis of the cycle topology of the covariance matrix, (SIII) calculations of responses of detailed balanced edges, and (SIV) calculations for the example of QDs, which includes Refs. [48–51].

[48] A. Wachtel, J. Vollmer, and B. Altaner, Phys. Rev. E **92**, 042132 (2015).

[49] M. Polettini, A. Lazarescu, and M. Esposito, Phys. Rev. E **94**, 052104 (2016).

[50] M. Polettini and M. Esposito, J. Stat. Phys. **176**, 94 (2019).

[51] M. Polettini and M. Esposito, Phys. Rev. Lett. **119**, 240601 (2017).

[52] N. Shiraishi and T. Sagawa, Phys. Rev. E **91**, 012130 (2015).

[53] J. Zheng and Z. Lu, arXiv:2403.10952.

[54] Using $\partial_{B_e} j_e = j_e$ with Eqs. (11) and (13) of [41] we arrive at $\sum_e d_{B_e} j_{e'} = j_{e'}$.

[55] A. Despons, Y. De Decker, and D. Lacoste, Commun. Phys. **7**, 224 (2024).

[56] S. Liang, P. De Los Rios, and D. M. Busiello, Phys. Rev. Lett. **132**, 228402 (2024).

[57] S. Liang, P. D. L. Rios, and D. M. Busiello, arXiv:2407.11498.

[58] A. Cottet, W. Belzig, and C. Bruder, Phys. Rev. B **70**, 115315 (2004).

[59] A. Cottet, W. Belzig, and C. Bruder, Phys. Rev. Lett. **92**, 206801 (2004).

[60] B. R. Bułka, Phys. Rev. B **62**, 1186 (2000).

[61] W. Belzig, Phys. Rev. B **71**, 161301(R) (2005).

[62] A. Y. Mitrophanov, J. Appl. Probab. **42**, 1003 (2005).

[63] V. Lucarini, J. Stat. Phys. **162**, 312 (2016).

[64] M. Santos Gutiérrez and V. Lucarini, J. Stat. Phys. **179**, 1572 (2020).

[65] G. Falasco, T. Cossetto, E. Penocchio, and M. Esposito, New J. Phys. **21**, 073005 (2019).

[66] J. D. Mallory, A. B. Kolomeisky, and O. A. Igoshin, Proc. Natl. Acad. Sci. U.S.A. **117**, 8884 (2020).

[67] J. A. Owen and J. M. Horowitz, Nat. Commun. **14,** 1280 (2023).

[68] G. Fernandes Martins and J. M. Horowitz, Phys. Rev. E **108,** 044113 (2023).

[69] H.-M. Chun and J. M. Horowitz, J. Chem. Phys. **158,** 174115 (2023).

[70] T. Aslyamov and M. Esposito, Phys. Rev. Lett. **132,** 037101 (2024).

[71] P. E. Harunari, S. Dal Cengio, V. Lecomte, and M. Polettini, Phys. Rev. Lett. **133,** 047401 (2024).

[72] C. Floyd, A. R. Dinner, and S. Vaikuntanathan, arXiv:2404.03798.

[73] D. Frezzato, J. Chem. Phys. **160,** 234111 (2024).

[74] C. Floyd, A. R. Dinner, A. Murugan, and S. Vaikuntanathan, arXiv:2409.05827.

[75] Q. Gao, H.-M. Chun, and J. M. Horowitz, Phys. Rev. E **105,** L012102 (2022).

[76] Q. Gao, H.-M. Chun, and J. M. Horowitz, Europhys. Lett. **146,** 31001 (2024).

[77] F. Khodabandehlou, C. Maes, and K. Netočný, arXiv:2412.05019.

[78] S. E. Harvey, S. Lahiri, and S. Ganguli, Phys. Rev. E **108,** 014403 (2023).

[79] A. Murugan, D. A. Huse, and S. Leibler, Phys. Rev. X **4,** 021016 (2014).

[80] A. Cornish-Bowden, *Fundamentals of Enzyme Kinetics* (John Wiley & Sons, New York, 2013).

[81] U. Seifert, Annu. Rev. Condens. Matter Phys. **10,** 171 (2019).

[82] C. Maes, Phys. Rep. **850,** 1 (2020).

[83] T. Van Vu and Y. Hasegawa, J. Phys. Conf. Ser. **1593,** 012006 (2020).

[84] B. Ertel, J. van der Meer, and U. Seifert, Phys. Rev. E **105,** 044113 (2022).

[85] A. Y. Mitrophanov, J. Appl. Probab. **40,** 970 (2003).

[86] J. Zheng and Z. Lu, arXiv:2501.01050.

[87] K. Ptaszynski, T. Aslyamov, and M. Esposito, arXiv:2412.10233.

[88] R. Bao and S. Liang, arXiv:2412.19602.

[89] K. Liu and J. Gu, Commun. Phys. **8,** 62 (2025).

[90] E. Kwon, H.-M. Chun, H. Park, and J. S. Lee, arXiv:2411.18108.

[91] T. Van Vu, PRX Quantum **6,** 010343 (2025).

[92] K. Liu and J. Gu, arXiv:2501.04895.

[93] J. L. Lebowitz and H. Spohn, J. Stat. Phys. **95,** 333 (1999).

[94] D. Andrieux and P. Gaspard, J. Stat. Mech. (2007) P02006.

[95] T. Aslyamov, F. Avanzini, E. Fodor, and M. Esposito, Phys. Rev. Lett. **131,** 138301 (2023).

End Matter

Appendix A: Derivation of covariance matrix and FRRs—Here, we find an exact expression for the covariance matrix $\mathbb{C}$ and then use it to derive the FRRs shown in Eqs. (5)–(8). To find $\mathbb{C}$, we use the scaled cumulant generating function method [48,93,94] and define the "tilted" matrix $\mathbb{W}^\phi(\boldsymbol{q})$ with nondiagonal elements $W_{ij}^\phi(\boldsymbol{q}) = \sum_e [W_{+e} \exp(q_e) \delta_{s(+e)j} \delta_{t(+e)i} + W_{-e} \exp(-q_e) \delta_{s(+e)i} \delta_{t(+e)j}]$ and diagonal elements the same as $\mathbb{W}$. It implies that $\mathbb{W}^\phi(\boldsymbol{0}) = \mathbb{W}$ is the rate matrix. We calculate the elements of $\mathbb{C}$ as

$$C_{ee'} = \frac{\partial}{\partial q_e} \frac{\partial}{\partial q_{e'}} \lambda(\boldsymbol{q})\bigg|_{\boldsymbol{q}=0}, \tag{A1}$$

where $\lambda(\boldsymbol{q})$ is eigenvalue of the matrix $\mathbb{W}^\phi(\boldsymbol{q})$ with the largest real part. In [47], Sec. SI, we calculate Eq. (A1) to derive an exact expression,

$$\mathbb{C} = \mathbb{P}\mathbb{T}\mathbb{P}^\mathsf{T}, \tag{A2}$$

with

$$\mathbb{P} = \mathbb{1} - \hat{\mathbb{\Gamma}}(\hat{\mathbb{M}}\hat{\mathbb{\Gamma}})^{-1}\hat{\mathbb{M}}, \tag{A3}$$

where the matrices $\hat{\mathbb{M}}$ and $\hat{\mathbb{\Gamma}}$, are defined for the oriented graph $\mathcal{G}$ describing the transitions (edges) $\mathcal{E}$ between the states (nodes) $\mathcal{S}$. Then, $\hat{\mathbb{M}} = [\delta_{nt(+e)} - \delta_{ns(+e)}]_{\{n \neq N, \forall e\}}$ is the (reduced) incidence matrix of

the graph $\mathcal{G}$ with the removed Nth node; and $\hat{\mathbb{\Gamma}} = [\Gamma_{en} - \Gamma_{eN}]_{\{\forall e, n \neq N\}}$ is defined by the scaled incidence matrix $\Gamma_{en} = W_{+e}\delta_{ns(+e)} - W_{-e}\delta_{nt(+e)}$. The matrix $\hat{\mathbb{M}}\hat{\mathbb{\Gamma}}$ is invertible; see proof in [41]; the matrix $\mathbb{P}$ is the projection matrix $\mathbb{P}^2 = \mathbb{P}$, which was studied in the context of the response theory [41].

Finally, we derive FRRs. The key object here is the matrix $\mathbb{P}$ that also defines the static response of $\mathcal{J}$ to perturbations of the arbitrary vector parameter $\boldsymbol{p} = (\ldots, p_i, \ldots)$ controlling the rates $\mathbb{W}(\boldsymbol{p})$. Indeed, following Ref. [41], we find

$$\nabla^\mathsf{T} \mathcal{J} = (\ldots, d_{p_i}\mathcal{J}, \ldots) = \boldsymbol{x}^\mathsf{T} \mathbb{P}\mathbb{G}, \tag{A4}$$

where $\mathbb{G} = [\partial_{p_i} j_e]_{\forall e, i \in \mathcal{P}}$ is the Jacobian defined in terms of the partial derivatives and which are known from the rates model $\mathbb{W}(\boldsymbol{p})$. If the number of parameters equals the number of edges and they are independent, the Jacobian is invertible ($\mathbb{G}^{-1}$ exists). Therefore, using Eqs. (4), (A2), and (A4), we find

$$\langle\!\langle \mathcal{J}, \mathcal{J}' \rangle\!\rangle = \boldsymbol{x}^\mathsf{T} \mathbb{P}\mathbb{G}\mathbb{G}^{-1}\mathbb{T}(\mathbb{G}^{-1})^\mathsf{T}(\boldsymbol{x}' \cdot \mathbb{P}\mathbb{G})^\mathsf{T}$$
$$= \boldsymbol{x}^\mathsf{T} \nabla_{\!p}^\mathsf{T} \boldsymbol{j} \cdot \mathbb{U} \cdot (\boldsymbol{x}'^\mathsf{T} \nabla_{\!p}^\mathsf{T} \boldsymbol{j})^\mathsf{T}, \tag{A5}$$

where the vector $\boldsymbol{x}^\mathsf{T} \nabla_{\!p}^\mathsf{T} \boldsymbol{j} = (\ldots, \sum_{e'} x_{e'} d_{p_e} j_{e'} \ldots,)$ and where

$$\mathbb{U} = \mathbb{G}^{-1}\mathbb{T}(\mathbb{G}^{-1})^{\mathsf{T}}. \tag{A6}$$

Equation (A5) is the general result at the core of FRRs. In general case, the vector $\mathbf{x}$ could be arbitrary implying that

$$d_{p_e}\mathcal{J} = \sum_{e'}(d_{p_e}x_{e'})j_{e'} + \sum_{e'}x_{e'}d_{p_e}j_{e'},$$

$$(\mathbf{x}^{\mathsf{T}}\nabla_h^{\mathsf{T}}\mathbf{j})_e = d_{p_e}\mathcal{J} - \Delta_e\mathcal{J}, \tag{A7}$$

where we introduced $\Delta_e\mathcal{J} = \sum_{e'}(d_{p_e}x_{e'})j_{e'}$, the response due to $d_{p_e}\mathbf{x}$. Inserting Eq. (A7) into Eq. (A5), we find the general form of FRR as

$$\langle\!\langle\mathcal{J},\mathcal{J}'\rangle\!\rangle = \sum_{e,e'}U_{ee'}(d_{p_e}\mathcal{J} - \Delta_e\mathcal{J})(d_{p_{e'}}\mathcal{J}' - \Delta_{e'}\mathcal{J}'). \tag{A8}$$

In the main text we assume that $\mathbf{x}$ does not depend on $\mathbf{p}$. Using $d_{p_e}\mathbf{x} = 0$ in Eq. (A8) we arrive at

$$\langle\!\langle\mathcal{J},\mathcal{J}'\rangle\!\rangle = \nabla^{\mathsf{T}}\mathcal{J}\mathbb{U}\nabla\mathcal{J}'. \tag{A9}$$

If $\mathbf{p} = (\dots, B_e, \dots)^{\mathsf{T}}$, we find $\mathbb{G} = \text{diag}(\dots, j_e, \dots)$ and $\mathbb{U} = \mathbb{D}^{-1}$, which gives Eqs. (5) and (6). If $\mathbf{p} = (\dots, S_e, \dots)^{\mathsf{T}}$, we find $\mathbb{G} = \mathbb{T}/2$ and $\mathbb{U} = 4\mathbb{T}^{-1}$, which gives Eqs. (7) and (8).

Appendix B: Application to chemical reactions—Here, we consider a simple example of chemical reaction networks shown in Fig. 2, where the network includes three internal chemical species, X_1, X_2, and X_3, interconverted by three reactions. One of these reactions is driven by the conversion of an external fuel, F, into waste, W. The concentrations of F and W, denoted c_F and c_W, respectively, are externally regulated using chemostats. In biological terms, F and W could represent ATP and ADP, respectively, and the system in Fig. 2 could be a simplified model of a molecular motor.

Assuming mass action law (the lack of molecular interaction between species [95]), the reaction currents read

$$\mathbf{j} = (k_{+1}\pi_1 c_F - k_{-1}\pi_2 c_W, k_{+2}\pi_2 - k_{-2}\pi_3, k_{+3}\pi_3 - k_{-3}\pi_1)^{\mathsf{T}}, \tag{B1}$$

where π_i is the scaled concentration of the component X_i such that $\sum_i \pi_i = 1$; $k_{\pm\rho} > 0$ are reaction constants for $\rho = 1, 2, 3$. In NESS, the system satisfies

$$\partial_t\boldsymbol{\pi} = \mathbb{W}\boldsymbol{\pi} = 0, \tag{B2a}$$

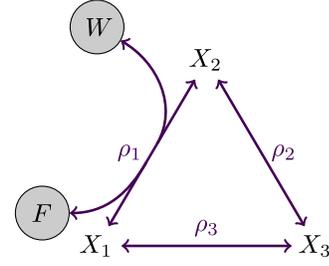$$\mathcal{J} = j_\rho \neq 0, \tag{B2b}$$

with

FIG. 2. An example of pseudounimolecular reactions $\rho \in \{1, 2, 3\}$; X_i are internal species, F and W are external (chemostatted) species.

$$\mathbb{W} = \begin{pmatrix} -k_{+1}c_F - k_{-3} & k_{-1}c_W & k_{+3} \\ k_{+1}c_F & -k_{-1}c_W - k_{+2} & k_{-2} \\ k_{-3} & k_{+2} & -k_{-2} - k_{+3} \end{pmatrix}, \tag{B3}$$

which plays the role of the rate matrix for the Markov jump processes corresponding to Fig. 2.

The symmetric and asymmetric parts of transition rate W_{+1} can be then expressed as $B_1 = \ln\sqrt{k_{+1}k_{-1}c_F c_W}$ and $S_1 = \ln[k_{+1}c_F/(k_{-1}c_W)]$. Consequently, using chain rule for derivatives, the response to symmetric and antisymmetric perturbations of the reaction $\rho = 1$ can be expressed explicitly in terms of current responses to concentrations (cf. Ref. [40]),

$$\frac{d\mathcal{J}}{dB_1} = c_F\frac{d\mathcal{J}}{dc_F} + c_W\frac{d\mathcal{J}}{dc_W}, \tag{B4a}$$

$$\frac{d\mathcal{J}}{dS_1} = \frac{1}{2}\left(c_F\frac{d\mathcal{J}}{dc_F} - c_W\frac{d\mathcal{J}}{dc_W}\right). \tag{B4b}$$

Inserting the above expressions into Eqs. (15) and (20), one can bound the entropy production and traffic of reaction $\rho = 1$, σ_1, and τ_1, measuring the current fluctuations $\langle\!\langle\mathcal{J}\rangle\!\rangle$ and empirical responses to concentrations c_F and c_W,

$$\dot{\sigma}_1 \geq \frac{2}{\langle\!\langle\mathcal{J}\rangle\!\rangle}\left(c_F\frac{d\mathcal{J}}{dc_F} + c_W\frac{d\mathcal{J}}{dc_W}\right)^2, \tag{B5a}$$

$$\tau_1 \geq \frac{1}{\langle\!\langle\mathcal{J}\rangle\!\rangle}\left(c_F\frac{d\mathcal{J}}{dc_F} - c_W\frac{d\mathcal{J}}{dc_W}\right)^2. \tag{B5b}$$

We emphasize that we only used the network topology and mass action law, and did not need to know the reaction constants $k_{\pm\rho}$.

In the case where the current $\mathcal{J}$ is known, Eq. (B5a) can be used to bound the edge affinity $\mathcal{A}_1 = \dot{\sigma}_1/\mathcal{J}$. Moreover, from Eqs. (B1) and (B2b), and $\tau_1 = k_{+1}\pi_1 c_F + k_{-1}\pi_2 c_W$ we further have $\tau_1 = 2c_F\pi_1 k_{+1} - \mathcal{J}$ and $\tau_1 = 2c_W\pi_2 k_{-1} + \mathcal{J}$. Inserting those expression into

Eq. (20) and using $\pi_i \leq 1$, we obtain bounds for reaction constants $k_{\pm 1}$,

$$k_{+1} \geq \frac{1}{2c_F} \left[\frac{4}{\langle\!\langle \mathcal{J} \rangle\!\rangle} \left(\frac{d\mathcal{J}}{dS_1} \right)^2 + \mathcal{J} \right], \qquad \text{(B6a)}$$

$$k_{-1} \geq \frac{1}{2c_W} \left[\frac{4}{\langle\!\langle \mathcal{J} \rangle\!\rangle} \left(\frac{d\mathcal{J}}{dS_1} \right)^2 - \mathcal{J} \right]. \qquad \text{(B6b)}$$

If the ratio k_{+1}/k_{-1} is known, one can bound the ratio of concentrations π_2/π_1 using the relation $\mathcal{A}_1 = \ln(k_{+1}c_F\pi_1/k_{-1}c_W\pi_2)$. Indeed, for the graph orientation with $\mathcal{J} > 0$, we find

$$\frac{\pi_1}{\pi_2} \geq \frac{k_{-1}c_W}{k_{+1}c_F} \exp\left[\frac{2}{\mathcal{J}\langle\!\langle \mathcal{J} \rangle\!\rangle} \left(c_F \frac{d\mathcal{J}}{dc_F} + c_W \frac{d\mathcal{J}}{dc_W} \right)^2 \right]. \qquad \text{(B7)}$$